



CHORUS

This is the accepted manuscript made available via CHORUS. The article has been published as:

Proper and improper chiral magnetic interactions

Manuel dos Santos Dias, Sascha Brinker, András Lászlóffy, Bendegúz Nyári, Stefan Blügel, László Szunyogh, and Samir Lounis

Phys. Rev. B **103**, L140408 — Published 23 April 2021

DOI: [10.1103/PhysRevB.103.L140408](https://doi.org/10.1103/PhysRevB.103.L140408)

Proper and improper chiral magnetic interactions

Manuel dos Santos Dias,^{1,*} Sascha Brinker,^{1,†} András Lászlóffy,^{2,3}
Bendegúz Nyári,³ Stefan Blügel,¹ László Szunyogh,^{3,4} and Samir Lounis^{1,5,‡}

¹*Peter Grünberg Institut and Institute for Advanced Simulation,
Forschungszentrum Jülich & JARA, 52425 Jülich, Germany*

²*Wigner Research Centre for Physics, P.O. Box 49, H-1525 Budapest, Hungary*

³*Department of Theoretical Physics, Budapest University of
Technology and Economics, Budafoki út 8, H-1111 Budapest, Hungary*

⁴*MTA-BME Condensed Matter Research Group, Budapest University of
Technology and Economics, Budafoki út 8, H-1111 Budapest, Hungary*

⁵*Faculty of Physics, University of Duisburg-Essen and CENIDE, 47053 Duisburg, Germany*

(Dated: March 29, 2021)

Atomistic spin models are of great value for predicting and understanding the magnetic properties of real materials, and extensions of the existing models open routes to new physics and potential applications. The Dzyaloshinskii-Moriya interaction is the prototype for chiral magnetic interactions, and several recent works have uncovered or proposed various types of generalized chiral interactions. However, in some cases the proposed interactions or their interpretation do not comply with basic principles such as being independent of the magnetic configuration from which they are evaluated, or even obeying time-reversal invariance. In this brief contribution, we present a simple explanation for the origin of these puzzling findings, and point out how to resolve them.

Introduction. The magnetic interaction between two spin moments is partitioned in isotropic, anisotropic, scalar and vector chiral interactions. The latter is commonly referred to as the chiral magnetic interaction and was developed by Dzyaloshinskii and Moriya [1, 2]. What is commonly understood by Dzyaloshinskii-Moriya interaction (DMI) is an antisymmetric exchange interaction that can be written for two spin moments as $\mathbf{D}_{12} \cdot (\mathbf{S}_1 \times \mathbf{S}_2)$. The interaction vector \mathbf{D}_{12} obeys the symmetry rules enumerated by Moriya [2]. Different microscopic mechanisms have been identified that lead to the DMI [2–6], all having in common the need for the relativistic spin-orbit interaction and an inversion asymmetric environment. The DMI underpins many interesting magnetic systems, such as weak ferromagnetism in antiferromagnets [1], spin spiral ground states [7], chiral magnetic domain walls [8], and magnetic skyrmions [9, 10].

With the advent of realistic electronic structure calculations, it became possible to compute the magnitude and other properties of the magnetic exchange interactions for a given material. A real-space approach to the pairwise interactions (the infinitesimal rotation method) was introduced in Ref. [11] and later generalized for the calculation of the DMI and other anisotropic interactions [12, 13]. The central idea is to establish a mapping between the electronic structure calculations and a suitably-defined atomistic spin model, but soon it was realized that this mapping is not trivial and can lead to a dependence of the computed interactions on the reference magnetic configuration [14–16]. A large part of these dependencies can be accounted for by expanding the reference atomistic spin model to include not only Heisenberg pairwise interactions but also biquadratic interactions [14, 15, 17], leading to generalized infinitesimal

rotation approaches to multi-spin interactions [18, 19].

A different approach consists in computing the energies of different magnetic configurations and parametrizing a spin model that can reproduce these energies. The general framework is called the spin cluster expansion and is easily applied to systematically map the complete set of interactions for a finite number of magnetic moments [20–23]. We have recently implemented the self-consistent spin cluster expansion within a constrained density functional theory framework [24, 25], leading to the identification of those four-spin interactions that are counterparts of the DMI: the chiral biquadratic interaction [24] in magnetic dimers, and its multi-site counterparts in trimers and tetramers [25], with some of these interactions not being constrained by Moriya’s rules. The significance of the chiral multi-spin interactions has also been recognized in [18, 26, 27].

Given the large interest in chiral magnetic interactions, we note that a few recent works have advanced unwarranted interpretations of otherwise sound first-principles calculations, such as chiral three-spin interactions that are incompatible with time-reversal symmetry [18], or a very large DMI [28, 29] that depends strongly on the magnetic configuration and does not rely on the spin-orbit interaction. The latter contradicts the understanding of the DMI as established by the magnetism community over the past 60 years, without offering a compelling theoretical justification for its revision. The purpose of this paper is to present a simple explanation for these proposed chiral interactions that we term ‘improper’, complying with basic symmetry requirements on the atomistic spin model.

Proper and improper magnetic interactions. Before we discuss our results, we define the terminology that we use

in this work. We term as ‘proper’ those magnetic interactions which are parametrized by interaction coefficients which are independent of the magnetic state of the system and are invariant under time-reversal symmetry (so they consist of an even number of spins), and if these properties are not satisfied we use the term ‘improper’. It is always possible to give a complete parametrization of the magnetic energy using only proper magnetic interactions [20–25]. For example, our analysis of a generic electronic model in Appendix B of Ref. [24] shows that only terms with an even number of magnetic moments appear in an infinite series expansion of the electronic grand potential (so no three-spin terms as advocated in Ref. [18]), and that terms containing only one explicit cross-product between them require the spin-orbit interaction (unlike the effective DMI of Refs. [28, 29]).

Improper DMI in Mn_3Sn . We start by reinterpreting the first-principles calculations performed for Mn_3Sn in Ref. [28]. This compound belongs to the space group $P6_3/mmc$ (194). The crystallographic unit cell shown in Fig. 1(a) consists of six Mn atoms that are partitioned into three ferromagnetic sublattices denoted by the indices $i, j \in \{1, 2, 3\}$. Each sublattice contains two atoms in the unit cell, one at $z = 1/4$ and one at $z = 3/4$. Ref. [28] computed the total energies for the family of magnetic configurations obtained when the magnetization for sublattices 2 and 3 are rotated by an angle $\pm\theta$ relative to that in sublattice 1. Hence, $\theta = 0^\circ$ denotes the ferromagnetic configuration, $\theta = 120^\circ$ denotes the triangular Néel configuration shown in Fig. 1(a), and $\theta = 180^\circ$ is a ferrimagnetic up-down-down state.

We repeated the total energy calculations of Ref. [28] employing the all-electron Korringa-Kohn-Rostoker Green function method in full potential [30] with spin-orbit coupling added to the scalar relativistic approximation [31]. We performed self-consistent calculations without constraints by treating exchange and correlation effects in the local spin density approximation [32]. We adopt the experimental lattice geometry following Ref. [33]. The scattering wave functions are expanded up to an angular momentum cutoff of $\ell_{\max} = 3$ and a k-mesh of $24 \times 24 \times 30$ is used. Our results shown in Fig. 1(b) are consistent with Ref. [28], exhibiting a pronounced fourth-order type energy behavior with respect to the rotation of the angle θ . Without spin-orbit interaction the antiferromagnetic triangular Néel states at $\theta = 120^\circ$ and $\theta = 240^\circ$ are degenerate. Including the spin-orbit interaction the well-known DMI emerges and the magnetic structure with Γ_5 symmetry corresponding to $\theta = 240^\circ$ is lower in energy by 8 meV than the one with Γ_3 symmetry denoted by $\theta = 120^\circ$, in agreement with the discussion of Ref. [34].

We depart from the analysis in Ref. [28] by fitting the dependence of our total energies on the magnetic configuration of the Mn sublattices i according to the extended

spin model that we presented in Refs. [25, 35], ($|\mathbf{S}_i| = 1$):

$$\begin{aligned} \mathcal{E} = & J_{12} (\mathbf{S}_1 \cdot \mathbf{S}_2 + \mathbf{S}_2 \cdot \mathbf{S}_3 + \mathbf{S}_3 \cdot \mathbf{S}_1) \\ & + B_{12} ((\mathbf{S}_1 \cdot \mathbf{S}_2)^2 + (\mathbf{S}_2 \cdot \mathbf{S}_3)^2 + (\mathbf{S}_3 \cdot \mathbf{S}_1)^2) \\ & + B_{123} ((\mathbf{S}_1 \cdot \mathbf{S}_2)(\mathbf{S}_2 \cdot \mathbf{S}_3) + (\mathbf{S}_2 \cdot \mathbf{S}_3)(\mathbf{S}_3 \cdot \mathbf{S}_1) \\ & \quad + (\mathbf{S}_3 \cdot \mathbf{S}_1)(\mathbf{S}_1 \cdot \mathbf{S}_2)) . \end{aligned} \quad (1)$$

Here we define the bilinear isotropic interaction between two sublattices with strength J_{12} , and two types of four-spin isotropic interactions between the sublattices: bi-quadratic with strength B_{12} and three-sublattice with strength B_{123} . Fig. 1(b) shows that the fit using only the bilinear two-sublattice interactions is quite poor, as claimed in Ref. [28], while inclusion of the four-spin two- and three-sublattice interactions fits the full angular dependence almost perfectly.

To see how the interpretation in terms of an improper Dzyaloshinskii-Moriya sublattice interaction can come about, we follow the strategy of Ref. [28] and derive the first-order change in the magnetic energy due to a small deviation of one of the spin directions for the spin model of Eq. (1). We replace $\mathbf{S}_1 \rightarrow \mathbf{S}_1 + \delta\mathbf{S}_1$ and find how the energy given by Eq. 1 changes due to this perturbation, with the result $\delta\mathcal{E}_1 = \delta\mathcal{E}_1^J + \delta\mathcal{E}_1^B$. The two contributions are

$$\delta\mathcal{E}_1^J = J_{12} (\mathbf{S}_2 + \mathbf{S}_3) \cdot \delta\mathbf{S}_1 \quad (2)$$

$$\delta\mathcal{E}_1^B = 2B_{12} ((\mathbf{S}_1 \cdot \mathbf{S}_2) \mathbf{S}_2 + (\mathbf{S}_3 \cdot \mathbf{S}_1) \mathbf{S}_3) \cdot \delta\mathbf{S}_1 . \quad (3)$$

The other four-spin interaction is discussed later. We have nothing to remark about $\delta\mathcal{E}_1^J$, but $\delta\mathcal{E}_1^B$ can be expressed in an alternative form using the vector identity

$$(\mathbf{A} \times \mathbf{B}) \cdot (\mathbf{C} \times \mathbf{D}) = (\mathbf{A} \cdot \mathbf{C})(\mathbf{B} \cdot \mathbf{D}) - (\mathbf{A} \cdot \mathbf{D})(\mathbf{B} \cdot \mathbf{C}) . \quad (4)$$

For small deviations $\mathbf{S}_1 \cdot \delta\mathbf{S}_1 = 0$, and we find

$$\begin{aligned} \delta\mathcal{E}_1^B = & 2B_{12} (\mathbf{S}_1 \times \mathbf{S}_2) \cdot (\mathbf{S}_2 \times \delta\mathbf{S}_1) \\ & + 2B_{12} (\mathbf{S}_1 \times \mathbf{S}_3) \cdot (\mathbf{S}_3 \times \delta\mathbf{S}_1) \\ = & \mathbf{D}_{21} \cdot (\mathbf{S}_2 \times \delta\mathbf{S}_1) + \mathbf{D}_{31} \cdot (\mathbf{S}_3 \times \delta\mathbf{S}_1) . \end{aligned} \quad (5)$$

These effective DM vectors are artificial, as they were obtained by rearranging the contribution from the isotropic four-spin sublattice interactions. Expanding their definition, e.g.

$$\mathbf{D}_{21} = 2B_{12} (\mathbf{S}_1 \times \mathbf{S}_2) = 2B_{12} \sin \theta \mathbf{z} = D_{21}(\theta) \mathbf{z} . \quad (6)$$

It follows that these effective DM vectors strongly depend on the magnetic configuration chosen for their calculation. They vanish for collinear magnetic configurations ($\theta = 0^\circ, 180^\circ$), have a maximum magnitude of $2B_{12} \approx 150$ meV, and do not arise from the spin-orbit interaction. Lastly, they are achiral, as chirality reversal is achieved by $\theta \rightarrow -\theta$ which leads to $D_{21}(-\theta) = -D_{21}(\theta)$,

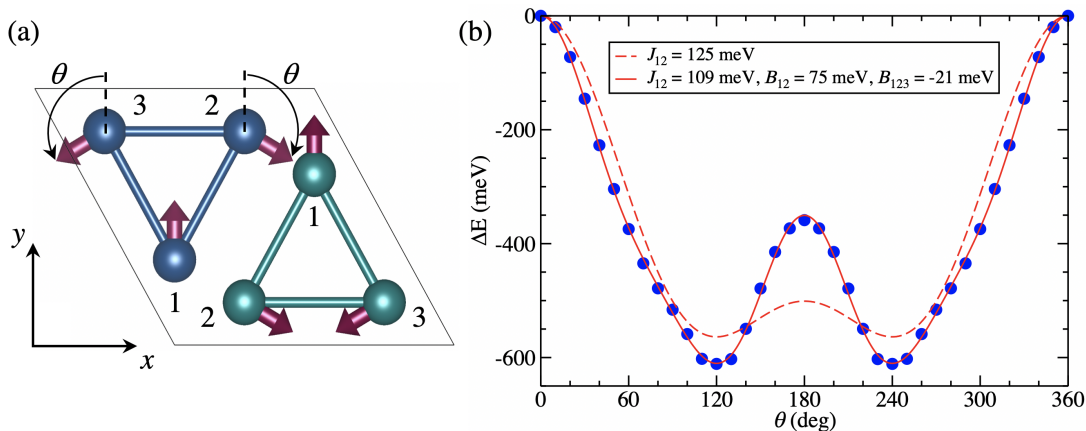


FIG. 1. Dependence of the total energy of Mn₃Sn on the magnetic configuration. (a) Top view of the unit cell of Mn₃Sn with noncollinear magnetic structure viewed along the z -axis. The spheres indicate the Mn atoms on the $z = 1/4$ plane (blue) and on the $z = 3/4$ plane (green). Sn is not shown. (b) Total energy for the magnetic configurations shown in (a) fitted to the spin model of Eq. (1) including only isotropic two-sublattice (J_{12}) or also biquadratic and three-sublattice interactions (B_{12} and B_{123} , respectively).

and so both chiralities have the same energy. All these properties match those reported in Ref. [28] including the magnitude of the interaction (see Fig. 3 within that reference), which points to isotropic four-spin sublattice interactions as the origin of the effective DMI proposed in that work.

Improper DMI in magnetic trimers. The authors of Ref. [28] have recently published a related work [29] which applies the same reasoning to magnetic Cr and Mn trimers on the Ag(111) and Au(111) surfaces. One methodological difference is that the improper DMI was computed by considering changes in two spins simultaneously, e.g. $\delta\mathbf{S}_1$ and $\delta\mathbf{S}_2$. Our spin model from Eq. (1) in combination with the vector identity of Eq. (4) leads to the second-order variations of the Heisenberg interaction

$$\delta\mathcal{E}_{12}^J = J_{12} \delta\mathbf{S}_1 \cdot \delta\mathbf{S}_2, \quad (7)$$

and of the biquadratic and three-site interactions

$$\begin{aligned} \delta\mathcal{E}_{12}^B &= 2B_{12} (\mathbf{S}_1 \cdot \mathbf{S}_2) (\delta\mathbf{S}_1 \cdot \delta\mathbf{S}_2) \\ &+ B_{123} (\mathbf{S}_1 + \mathbf{S}_2) \cdot \mathbf{S}_3 (\delta\mathbf{S}_1 \cdot \delta\mathbf{S}_2) \\ &+ 2B_{12} (\mathbf{S}_1 \times \mathbf{S}_2) \cdot (\delta\mathbf{S}_2 \times \delta\mathbf{S}_1) \\ &+ B_{123} (\mathbf{S}_1 \times \mathbf{S}_3 + \mathbf{S}_3 \times \mathbf{S}_2) \cdot (\delta\mathbf{S}_2 \times \delta\mathbf{S}_1) \\ &+ B_{123} (\delta\mathbf{S}_1 \cdot \mathbf{S}_3) (\mathbf{S}_3 \cdot \delta\mathbf{S}_2). \end{aligned} \quad (8)$$

The first and second lines are contributions to an effective Heisenberg-like interaction, the third and fourth lines to an improper DMI-like interaction, and the last line to an artificial Ising-like interaction. This shows that the effective interactions obtained by varying two spin orientations can also generate contributions which are hard to interpret without comparing to an appropriate spin model, and can depend not only on the spin alignment for the pair of interest (spins 1 and 2) but also on how they

align with the rest of the system (spin 3). We propose that these interactions explain the very large improper DMI reported in Table 2 of Ref. [29] in contrast with the proper one driven by the spin-orbit interaction.

Unfortunately, a direct quantitative comparison between Ref. [29] and our published results for Cr and Mn trimers on Au(111) in [22] and [25] is not possible due to large computational differences. For the benefit of the reader, we note that the magnetic interactions were evaluated in Ref. [22] by fitting the energies of a large number of magnetic configurations in combination with the magnetic force theorem, while in [25] they were fitted to the self-consistent constraining fields stabilizing a selected number of symmetry-inequivalent magnetic configurations. For a quick comparison between the magnitudes of the proper and improper DMI using our own results, we select the Cr trimer on Au(111) and adopt the triangular Néel state. In the notation of [25], the z -component of the improper DMI for this magnetic configuration is $D_{z1}^z = \sqrt{3} (B_{12} - B_{123})$, which amounts to -20 meV [22] or -23 meV [25]. The improper DMI is much larger than the proper DMI, 0.97 meV [22] or 1.7 meV [25], but still more than six times smaller than the value of 134 meV reported by Ref. [28]. We find it hard to explain such a large discrepancy solely with computational differences between our two works and Ref. [28]. As Refs. [22] and [25] use a systematic mapping of the energy as a function of the magnetic configuration, such a large missing contribution to the energy would have been noticed.

We now look at the dependence of the artificial DMI on a different set of magnetic configurations [25, 29], as

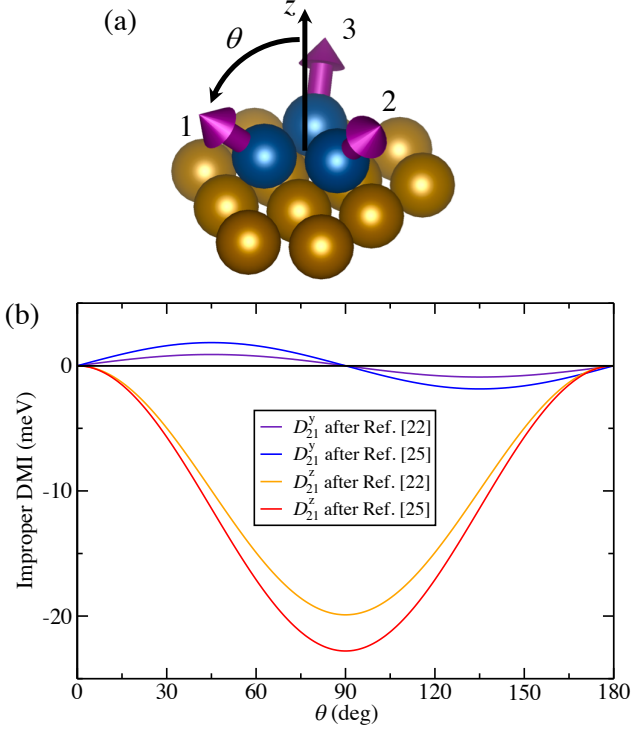


FIG. 2. Dependence of the improper DMI on the magnetic configuration for a Cr trimer on Au(111). (a) Noncollinear magnetic structure. The blue spheres represent Cr atoms and the golden spheres Au atoms. (b) Dependence of the improper DMI between atoms 1 and 2 due to isotropic four-spin interactions on the magnetic configuration, according to Eq. (10) and the parameters $B_{12} = -4.42$ meV and $B_{123} = 7.06$ meV from Ref. [22] and $B_{12} = -5.10$ meV and $B_{123} = 8.06$ meV from Ref. [25].

illustrated in Fig. 2(a):

$$\mathbf{S}_1 = \left(\frac{\sqrt{3}}{2} \sin \theta, \frac{1}{2} \sin \theta, \cos \theta \right), \quad (9a)$$

$$\mathbf{S}_2 = \left(-\frac{\sqrt{3}}{2} \sin \theta, \frac{1}{2} \sin \theta, \cos \theta \right), \quad (9b)$$

$$\mathbf{S}_3 = (0, -\sin \theta, \cos \theta). \quad (9c)$$

These keep the threefold rotation symmetry about the z -axis. Here $\theta = 0^\circ$ is a ferromagnetic arrangement with the spin moments pointing along $+z$, $\theta = 90^\circ$ is the triangular Néel configuration, and $\theta = 180^\circ$ is a ferromagnetic arrangement with the spin moments pointing along $-z$. The improper DMI for a representative pair follows from Eq. (8) and the chosen magnetic configuration:

$$D_{21}^y(\theta) = -\sqrt{3} \left(B_{12} + \frac{1}{2} B_{123} \right) \sin 2\theta, \quad (10a)$$

$$D_{21}^z(\theta) = \sqrt{3} (B_{12} - B_{123}) \sin^2 \theta. \quad (10b)$$

This shows that the same isotropic four-spin interactions can lead to different components of the improper DMI,

depending on the reference magnetic configuration. The angular dependence of the improper DMI is shown in Fig. 2(b), using the data from Refs. [22, 25].

Improper three-spin chiral interactions. We have argued so far that isotropic four-spin interactions can be misleadingly interpreted as improper chiral interactions. However, we have recently identified proper chiral four-spin interactions in several independent works [25–27], so we now explain how they fit the story. The concept of effective two-spin interactions is useful to characterize the local energy landscape around a reference magnetic configuration. In this context, the isotropic four-spin interaction can be shown to renormalize the isotropic Heisenberg interaction while the chiral four-spin interactions renormalize the conventional DMI [25].

These chiral four-spin interactions can also explain the improper chiral three-spin interactions introduced in Ref. [18]. There the infinitesimal rotation method was extended to a multi-spin multi-site framework, which among other things was used to identify the energy change from introducing spin deviations on three distinct sites. We stress that we do not doubt the numerical results of Ref. [18], but point out that their proposed interpretation with a chiral three-spin three-site interaction built out of the scalar spin chirality of the perturbed moments, $\delta \mathbf{S}_1 \cdot (\delta \mathbf{S}_2 \times \delta \mathbf{S}_3)$, is manifestly inconsistent with time-reversal symmetry. They remedied this inconsistency by defining a magnetic-configuration-dependent interaction strength, in a way similar to the previously-discussed improper DMI. The origin of these improper three-spin interactions can be found by starting from the form of the chiral four-spin interactions given in Ref. [27],

$$\mathcal{E}^C = (\mathbf{C}_{123} \cdot \mathbf{S}_1) \mathbf{S}_1 \cdot (\mathbf{S}_2 \times \mathbf{S}_3) + \dots \quad (11)$$

The dots denote other terms obtained by permutations of $\{1, 2, 3\}$. Note that this form of a chiral three-site interaction incorporates some symmetries of the underlying lattice and cannot describe the general case as discussed in Ref. [25]. If we introduce small deviations of the three spin orientations simultaneously, we arrive at

$$\Delta \mathcal{E}_{123}^C = (\mathbf{C}_{123} \cdot \mathbf{S}_1) \delta \mathbf{S}_1 \cdot (\delta \mathbf{S}_2 \times \delta \mathbf{S}_3) + \dots \quad (12)$$

$$= J_{123}^{(1)} \delta \mathbf{S}_1 \cdot (\delta \mathbf{S}_2 \times \delta \mathbf{S}_3) + \dots \quad (13)$$

where $J_{123}^{(1)}$ is a contribution to the chiral three-spin interaction coefficient in the notation of Ref. [18]. It depends on the proper chiral four-spin interaction vector \mathbf{C}_{123} [25–27] and how the reference magnetic configuration is aligned with it. We see no reason to introduce and use such improper chiral three-spin interactions when the proper chiral four-spin ones have already been uncovered and described. Surprisingly, the authors of Ref. [18] also acknowledge this in practice, as stated in the text following Eq. 29 within that work.

Conclusions. We showed how isotropic four-spin interactions can be misinterpreted as improper DMI-like interactions that have very pathological properties, chiefly being strongly dependent on the reference magnetic configuration used in the calculation. The ‘natural’ choice of a collinear ferromagnetic state as the reference state avoids most of these problems due to all magnetic moments being collinear. Great care must be exercised in interpreting the results of the infinitesimal rotation approach if the reference state is not collinear, and we propose that for this to be successful the appropriate spin model must be defined beforehand in accordance with all the symmetries of the material (see Ref. [25] for a detailed discussion). Lastly, we remark that improper chiral three-spin three-site interactions can likewise be obtained from varying the orientations of three magnetic moments and misinterpreting the result [18]. These arise from proper chiral four-spin interactions [25–27], which interestingly were also identified in Ref. [18], and acquire a dependence on the magnetic configuration through the orientation of the undisturbed fourth spin.

Acknowledgements. We gratefully acknowledge financial support from the DARPA TEE program through grant MIPR (# HR0011831554) from DOI, from the European Research Council (ERC) under the European Union’s Horizon 2020 research and innovation program (Grant No. 856538, project “3D MAGiC” and ERC-consolidator grant 681405 — DYNASORE), from Deutsche Forschungsgemeinschaft (DFG) through SPP 2137 “Skyrmionics” (Project BL 444/16), Priority Programme SPP 2244 “2D Materials - Physics of van der Waals Heterostructures” (project LO 1659/7-1), and the Collaborative Research Centers SFB 1238 (Project C01). B.N., A.L. and L.S. acknowledge the support provided by the Ministry of Innovation and the National Research, Development, and Innovation (NRDI) Office under Project No. K131938, by the NRDI Fund (TKP2020 IES, Grant No. BME-IE-NAT) and within the Quantum Information National Laboratory of Hungary. The authors gratefully acknowledge the computing time granted through JARA-HPC on the supercomputer JURECA at the Forschungszentrum Jülich [36].

* m.dos.santos.dias@fz-juelich.de

† s.brinker@fz-juelich.de

‡ s.lounis@fz-juelich.de

- [1] I. E. Dzyaloshinskii, “Thermodynamic theory of “weak” ferromagnetism in antiferromagnetic substances,” *Sov. Phys. JETP* **5**, 1259 – 1272 (1957).
- [2] Toru Moriya, “Anisotropic superexchange interaction and weak ferromagnetism,” *Phys. Rev.* **120**, 91–98 (1960).
- [3] D.A. Smith, “New mechanisms for magnetic anisotropy in localised s-state moment materials,” *J. Magn. Magn. Mater.* **1**, 214 – 225 (1976).
- [4] A. Fert and Peter M. Levy, “Role of anisotropic exchange interactions in determining the properties of spin-glasses,” *Phys. Rev. Lett.* **44**, 1538–1541 (1980).
- [5] Hiroshi Imamura, Patrick Bruno, and Yasuhiro Utsumi, “Twisted exchange interaction between localized spins embedded in a one- or two-dimensional electron gas with Rashba spin-orbit coupling,” *Phys. Rev. B* **69**, 121303(R) (2004).
- [6] Toru Kikuchi, Takashi Koretsune, Ryotaro Arita, and Gen Tatara, “Dzyaloshinskii-Moriya interaction as a consequence of a Doppler shift due to spin-orbit-induced intrinsic spin current,” *Phys. Rev. Lett.* **116**, 247201 (2016).
- [7] Matthias Bode, M Heide, K Von Bergmann, P Ferriani, S Heinze, G Bihlmayer, A Kubetzka, O Pietzsch, S Blügel, and R Wiesendanger, “Chiral magnetic order at surfaces driven by inversion asymmetry,” *Nature* **447**, 190–193 (2007).
- [8] Satoru Emori, Uwe Bauer, Sung-Min Ahn, Eduardo Martinez, and Geoffrey SD Beach, “Current-driven dynamics of chiral ferromagnetic domain walls,” *Nature Materials* **12**, 611–616 (2013).
- [9] Naoto Nagaosa and Yoshinori Tokura, “Topological properties and dynamics of magnetic skyrmions,” *Nat. Nanotechnol.* **8**, 899–911 (2013).
- [10] Albert Fert, Nicolas Reyren, and Vincent Cros, “Magnetic skyrmions: advances in physics and potential applications,” *Nature Reviews Materials* **2**, 201731 (2017).
- [11] A Il Liechtenstein, MI Katsnelson, VP Antropov, and VA Gubanov, “Local spin density functional approach to the theory of exchange interactions in ferromagnetic metals and alloys,” *J. Magn. Magn. Mater.* **67**, 65–74 (1987).
- [12] Laszlo Udvardi, Laszlo Szunyogh, K Palotás, and Peter Weinberger, “First-principles relativistic study of spin waves in thin magnetic films,” *Phys. Rev. B* **68**, 104436 (2003).
- [13] H Ebert and S Mankovsky, “Anisotropic exchange coupling in diluted magnetic semiconductors: Ab initio spin-density functional theory,” *Phys. Rev. B* **79**, 045209 (2009).
- [14] Samir Lounis and Peter H. Dederichs, “Mapping the magnetic exchange interactions from first principles: Anisotropy anomaly and application to Fe, Ni, and Co,” *Phys. Rev. B* **82**, 180404(R) (2010).
- [15] Attila Szilva, M Costa, Anders Bergman, L Szunyogh, Lars Nordström, and Olle Eriksson, “Interatomic exchange interactions for finite-temperature magnetism and nonequilibrium spin dynamics,” *Phys Rev Lett* **111**, 127204 (2013).
- [16] A. Szilva, D. Thonig, P. F. Bessarab, Y. O. Kvashnin, D. C. M. Rodrigues, R. Cardias, M. Pereiro, L. Nordström, A. Bergman, A. B. Klautau, and O. Eriksson, “Theory of noncollinear interactions beyond Heisenberg exchange: Applications to bcc Fe,” *Phys. Rev. B* **96**, 144413 (2017).
- [17] O. N. Mryasov, A. J. Freeman, and A. I. Liechtenstein, “Theory of non-Heisenberg exchange: Results for localized and itinerant magnets,” *J. Appl. Phys.* **79**, 4805–4807 (1996).
- [18] S. Mankovsky, S. Polesya, and H. Ebert, “Extension of the standard Heisenberg Hamiltonian to multispin exchange interactions,” *Phys. Rev. B* **101**, 174401 (2020).

- [19] Samir Lounis, “Multiple-scattering approach for multi-spin chiral magnetic interactions: application to the one- and two-dimensional Rashba electron gas,” *New Journal of Physics* **22**, 103003 (2020).
- [20] R Drautz and M Fähnle, “Spin-cluster expansion: parametrization of the general adiabatic magnetic energy surface with ab initio accuracy,” *Physical Review B* **69**, 104404 (2004).
- [21] Ralf Drautz and Manfred Fähnle, “Parametrization of the magnetic energy at the atomic level,” *Physical Review B* **72**, 212405 (2005).
- [22] A Antal, B Lazarovits, L Udvardi, L Szunyogh, B Újfalussy, and P Weinberger, “First-principles calculations of spin interactions and the magnetic ground states of Cr trimers on Au(111),” *Phys. Rev. B* **77**, 174429 (2008).
- [23] R. Singer, F. Dietermann, and M. Fähnle, “Spin interactions in bcc and fcc Fe beyond the Heisenberg model,” *Phys. Rev. Lett.* **107**, 017204 (2011).
- [24] Sascha Brinker, Manuel dos Santos Dias, and Samir Lounis, “The chiral biquadratic pair interaction,” *New J. Phys.* **21**, 083015 (2019).
- [25] Sascha Brinker, Manuel dos Santos Dias, and Samir Lounis, “Prospecting chiral multisite interactions in prototypical magnetic systems,” *Phys. Rev. Research* **2**, 033240 (2020).
- [26] A. Lászlóffy, L. Rózsa, K. Palotás, L. Udvardi, and L. Szunyogh, “Magnetic structure of monatomic Fe chains on Re(0001): Emergence of chiral multispin interactions,” *Phys. Rev. B* **99**, 184430 (2019).
- [27] S. Grytsiuk, J.-P. Hanke, M. Hoffmann, J. Bouaziz, O. Gomonay, G. Bihlmayer, S. Lounis, Y. Mokrousov, and S. Blügel, “Topological-chiral magnetic interactions driven by emergent orbital magnetism,” *Nat. Commun.* **11**, 511 (2020).
- [28] Ramon Cardias, Anders Bergman, Attila Szilva, Yaroslav O. Kvashnin, Jonas Fransson, Angela B. Klautau, Olle Eriksson, and Lars Nordström, “Dzyaloshinskii-Moriya interaction in absence of spin-orbit coupling,” (2020), [arXiv:2003.04680](https://arxiv.org/abs/2003.04680) [cond-mat.mtrl-sci].
- [29] R. Cardias, A. Szilva, M. M. Bezerra-Neto, M. S. Ribeiro, A. Bergman, Y. O. Kvashnin, J. Fransson, A. B. Klautau, O. Eriksson, and L. Nordström, “First-principles Dzyaloshinskii-Moriya interaction in a non-collinear framework,” *Sci. Rep.* **10**, 20339 (2020).
- [30] N. Papanikolaou, R. Zeller, and P. H. Dederichs, “Conceptual improvements of the KKR method,” *Journal of Physics: Condensed Matter* **14**, 2799–2823 (2002).
- [31] D. S. G. Bauer, *Development of a relativistic full-potential first-principles multiple scattering Green function method applied to complex magnetic textures of nano structures at surfaces*, Ph.D. thesis, RWTH Aachen (2014).
- [32] SH Vosko, L Wilk, and M Nusair, “Accurate spin-dependent electron liquid correlation energies for local spin density calculations: a critical analysis,” *Can. J. Phys.* **58**, 1200–1211 (1980).
- [33] Shōichi Tomiyoshi, “Polarized neutron diffraction study of the spin structure of Mn_3Sn ,” *Journal of the Physical Society of Japan* **51**, 803–810 (1982).
- [34] B. Nyári, A. Deák, and L. Szunyogh, “Weak ferromagnetism in hexagonal Mn_3Z alloys ($Z = Sn, Ge, Ga$),” *Phys. Rev. B* **100**, 144412 (2019).
- [35] Markus Hoffmann and Stefan Blügel, “Systematic derivation of realistic spin models for beyond-Heisenberg solids,” *Phys. Rev. B* **101**, 024418 (2020).
- [36] Jülich Supercomputing Centre, “JURECA: Modular supercomputer at Jülich Supercomputing Centre,” *Journal of large-scale research facilities* **4** (2018), 10.17815/jlsrf-4-121-1.